RF pulsed tests on 3GHZ niobium cavities

J. Le Duff, C. Thomas, G. Bienvenu, H. Sun, M. Fouaidy, R. Parodi

RF PULSED TESTS ON 3GHZ NIOBIUM CAVITIES

J. Le Duff, C. Thomas*, G. Bienvenu, H.Sun† LAL, Orsay, France
M. Fouaidy, IPN, Orsay, France , R. Parodi, INFN, Genova, Italy

Abstract

The achievable limiting RF field for S-Band and L-Band superconducting cavities is still an open question today. Previous studies on Sn and In have shown that a surface magnetic field B_s higher than the thermodynamical critical field B_c might be reached. The ultimate limiting field is then the superheating field B_{sh} (B_{sh} = 240 mT or E_{acc} = 60 MV/m for Nb at T= 0 K). However, the maximum accelerating field observed so far is in the range E_{acc} = 37-40 MV/m for the best 1.3 GHz Nb cavities. A dedicated facility (NEPAL Supra Test Facilty) is currenly used at LAL for measuring B_{sh} on bulk Nb 3 GHz cavities supplied by INFN-Genova. High power pulses (4.5 μs, up to 5 MW) are used to reach B_{sh} before cavity thermal breakdown occurs. A method for analyzing the response of a SRF cavity when subjected to pulsed high RF power was developed and the corresponding numerical simulation results were validated by comparison to experimental data. This technique is successfully applied to detect E_{acc} and B_{sh} at which the cavity magnetic breakdown occurs. Magnetic penetration depth (λ) measurements were also performed with a low RF level test bed and the corresponding data analyzed then compared to theoretical predictions.

1 INTRODUCTION

The maximum achieved accelerating fields in SRF cavities are usually limited by field emission and thermal breakdown. These two limits have been pushed back thanks to improvements of niobium purity, cavity preparation, assembling and conditionning techniques. In principle, a theoretical limit of the surface field higher than B_c (i.e B_c = 200 mT or 50MV/m accelerating field E_{acc} for TESLA shape bulk niobium (Nb) cavities at T = 0 K) is expected in CW mode of operation. Previous RF measurements performed on indium and tin samples and the corresponding theoretical estimation have shown that $B_s \geq B_c$ might be reached [1]. Moreover, the fundamental limit B_{sh} of bulk Nb is now close to being reached [2]. Due to lack of sufficient experimental data on B_{sh} for Nb, it is important to measure this parameter precisely.

2 SUPERHEATING FIELD AND PENETRATION DEPTH

In this section, we briefly summarize the useful relationships dealing with the predictions of B_{sh} and λ according to different theories.

* Email: cthomas@lal.in2p3.fr
† visitor, IHEP, Beijing, PRC

2.1 Superheating Field

For Type-II superconductors such as niobium, subjected to an external magnetic field B_a (static or slowly varying), the Meissner effect persists up to the first critical field, B_{c1}. For B_a lying between B_{c1} and B_{c2}, normal conducting areas are nucleated : this thermodynamic state is called the mixed state. Beyond B_{c2}, superconductivity is completely destroyed. Moreover, in the case of non-zero B_a, the transition from superconducting to normal conducting state is of first order. In this case, superheating is possible and a magnetic field (B_{sh}) higher than the critical field B_{c1} could then be sustained by the superconducting material. The superheating field B_{sh} is related to the critical thermodynamic field B_c. According to Ginzburg-Landau (GL) theory [3], we distinguish two kinds of superconductors depending on the value of the material's GL parameter $\kappa_{GL} = \frac{\lambda_{GL}}{\xi_{GL}}$ where ξ_{GL} is the GL coherence length:

For type I superconductors, $B_{sh} \approx \frac{0.89}{\sqrt{\kappa_{GL}}} B_c$.

For type II, $B_{sh} \approx 0.75 B_c$.

Note that niobium, which is a type II superconductor but with a peculiar behaviour due to a κ value close to the critical value $\kappa_{GL}^{Nb} \simeq \kappa_{GL}^{c} = \frac{1}{\sqrt{2}}$, we have :

$$B_{sh} = 1.2 * B_c \tag{1}$$

2.2 Penetration depth

The London magnetic penetration depth $\lambda_L(0)$ at absolute zero is given, according to the well-known phenomenological London theory, by $\lambda_L(0) = \sqrt{\frac{m}{\mu_0 n_s e^2}}$ where m, e are respectively the mass and charge of the electron and n_s is the density per unit volume of super electrons at T = 0 K. The temperature dependence of the cooper pair density, introduced in the two fluid model by Gorter-Casimir (GC), results in an empirical temperature-dependent London penetration depth : $\lambda_{GC}(t) = \lambda_{L0} \frac{1}{\sqrt{1-t^4}}$, where t is the reduced temperature ($t = T/T_c$) with reference to the material critical temperature T_c. This expression was derived in the London limit where $\xi_0 \gg \lambda$ and is not valid in the neighbourhood of T_c (i.e t close to 1) [4]. Ginzburg and Landau [3] showed that the penetration depth depends on the material purity, or equivalently the electron mean free path, leading to the following asymptotic expressions :

- for "clean" superconductors ($l \gg \xi_0$)

$$\lambda_{GL}(t) = \frac{\lambda_L(0)}{\sqrt{2(1-t)}} \tag{2}$$

- for "dirty" superconductors ($l \ll \xi_0$)

$$\lambda_{GL}(t) = \frac{\lambda_L(0)}{\sqrt{2}} \sqrt{\frac{\xi_0}{1.33 l}} \frac{1}{\sqrt{(1-t)}} \tag{3}$$

0-7803-5573-3/99/$10.00@1999 IEEE.

where ξ_0 is the BCS coherence length and l the mean free path of a normal electron. Note that measuring the magnetic penetration depth allow us to determine l and to obtain the RRR of our cavity in-situ. Direct RRR measurements on cavities [5] will be used to cross-check the first results. Moreover, we plan to measure both B_{sh} and λ (Eq. 3) before and after cavity heat treatment with Ti gettering (i.e material purification), hence we will be able to check the validity of the relationship given by Eq. 1 (i.e. B_{sh} doesn't depend on κ_{GL}).

3 METHOD OF B_{SH} MEASUREMENT

In most case, the maximum accelerating field is limited, in DC or long RF pulsed mode ($1-10$ms) by cavity thermal breakdown. To circumvent this problem, we use RF pulses of duration $\tau_p = 1-4.5\mu$s which are much shorter than the characteristic time needed for cavity thermal breakdown or quench induced by anomalous RF losses to occur ($\simeq 100\mu$s [6]). In order to achieve a good transfer efficiency between the RF source and the cavity, a strong external coupling is needed (i.e $Q_{ext} = 5.10^4$). As long as the cavity is in the superconducting state ($Q_0(4.2K) \simeq 7.10^7$), the cavity decay time $\tau = \frac{Q_L}{\omega}$, where Q_L is the loaded quality factor, is dominated by the external coupling (i.e $\tau \simeq \frac{Q_{ext}}{\omega}$). When a thermal or magnetic breakdown occurs, Q_0 jumps instantaneously to 10^6-10^5 and consequently τ decreases. The transmitted power integral $U_t = \int A \exp -\frac{t}{\tau} dt$, which is proportional to the incident power integral U_i, when the cavity is in the superconducting state, shows a deviation from the linear behaviour when the cavity quenches (i.e transition to the normal state) as illustrated in Fig. 1. The point, where such a deviation (eq. jump of U_t) is initiated and referred to as "B" in this figure, corresponds exactly to the quench field. Note that other methods of quench field measurements are not appropriate to our test stand [7].

4 EXPERIMENTAL APPARATUS AND PRELIMINARY RESULTS

In order to reach a high accelerating field, we use a 3 GHz-35 MW klystron with a maximum pulse length of 4.5μs. The experimental set-up block diagram is shown in Fig. 2. Data acquisition of all the experimental parameters and processing (RF signal integration) is performed using a dedicated Labview^{TM} program.

Experimental runs were performed and the corresponding preliminary results are displayed in Fig. 3. The shape of the experimental curve is close to the expected simulation results (see Fig. 1). More precisely , we clearly observe a linear part of U_t versus U_i up to a critical value of U_i ($U_i^c \simeq 1.4-1.5$ J). Moreover as expected, at this value U_t decreases sharply (cavity magnetic breakdown) when U_i is slightly increased, reaching a plateau at $U_t \simeq 0.6\mu$J for $U_i \geq 1.5$ J. Note that a precise value of the maximum E_{acc} and hence B_s at which the cavity magnetic breakdown occurs could not be deduced from these results at the time being because of some calibration uncertainties.

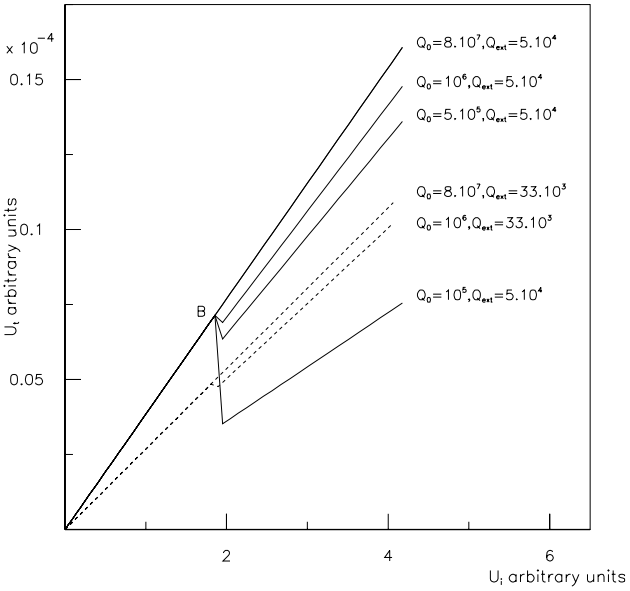

Figure 1: Simulation of the variation of the transmitted power integral versus the incident power integral.

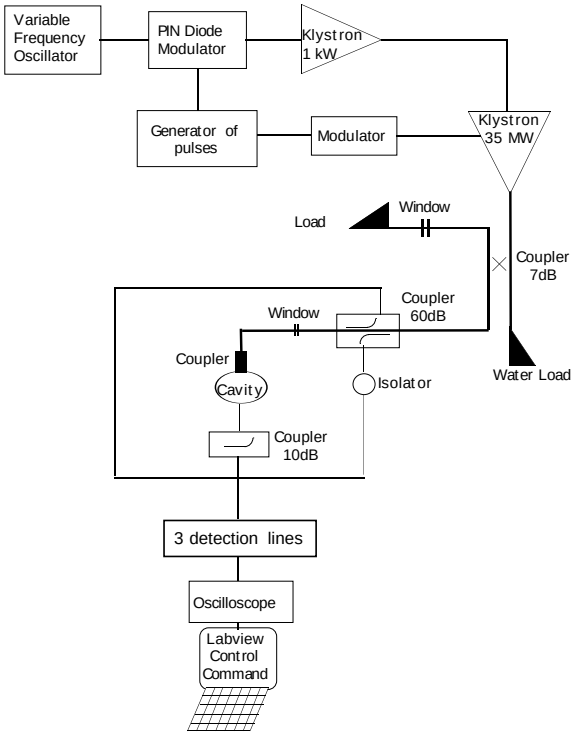

Figure 2: Schematic of experimental set-up

5 MAGNETIC PENETRATION DEPTH : METHOD AND RESULTS

The cavity resonant frequency is influenced by the magnetic penetration depth which is a temperature dependent parameter. More precisely, the reactive component of the cavity surface impedance X is related to the resonant fre-

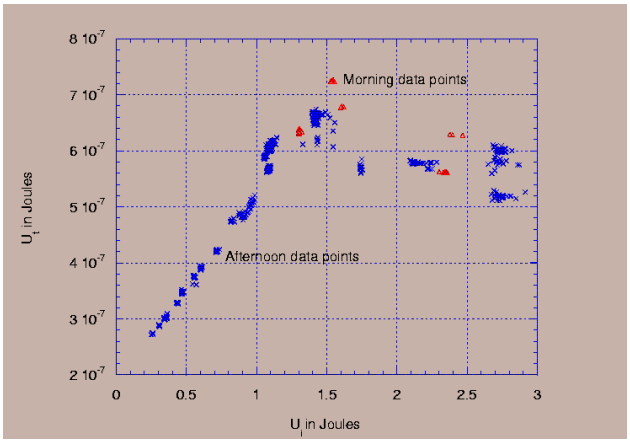

Figure 3: Integral of transmitted power versus integral of incident power (performed at T = 4.2 K on cavity CAT2)

quency f by the formula : $X = 2G\frac{(f-f_0)}{f_0}$ where G is the geometric factor and f_0 is the frequency of an ideal cavity (perfectly conducting). Moreover, X is proportional to the frequency and magnetic penetration depth ($X = 2\pi f \mu_0 \lambda$). Consequently, starting at an initial temperature $T_0 = 4.2K$ and recording the cavity frequency shift due to temperature variation, we can easily deduce the corresponding $\Delta\lambda$:

$$\Delta\lambda(T) = \lambda(T) - \lambda(T_0) = \frac{G}{\pi\mu_0}\frac{\Delta f}{f(T_0)^2} \qquad (4)$$

This procedure was used and the corresponding data (160 data points) analysed and compared (Fig. 4) to the theoretical relationships of GL (Eq. 3) or GC. These results clearly show that GL theory fits the data better than the GC theory : the corresponding mean standard deviation are respectively 23.1nm and 22.2nm for GC and GL theories. Note that the two fitting parameters are very sensitive to the Nb critical temperature T_c (T_c was ajusted by trial and error in the range : 9.1 K-9.4 K), and the optimum value was 9.3 K. This figure is close to published data ($T_c = 9.3$ K) [8]. The measured $\lambda_{GL}(4.2K) = 33$nm is in good agreement with previous results [9] leading to a mean free path l = 670 Å and hence a Residual Resistivity Ratio RRR = 10. The estimated RRR obtained from Nb impurities contents (O, C, N) [10] is 40. The apparent discrepency between the RRR deduced from λ_{GL} and the estimated one could be explained by RRR decrease near the Nb surface [11]. Finally, the corresponding experimental GL parameter is $\kappa_{GL}^{exp} = 1.1$ which is close to κ_{GL}^{c}.

6 ACKNOWLEDGEMENTS

We would like to thank J.N.Cayla for his technical support, G.Arnaud, Ph.Dufresne and M.Roch for their assistance concerning vacuum and cryogenics as well as the IPN Superconducting cavity group and S.Buhler for their helpful advice. A special thank to B.Mouton for his friendly help.

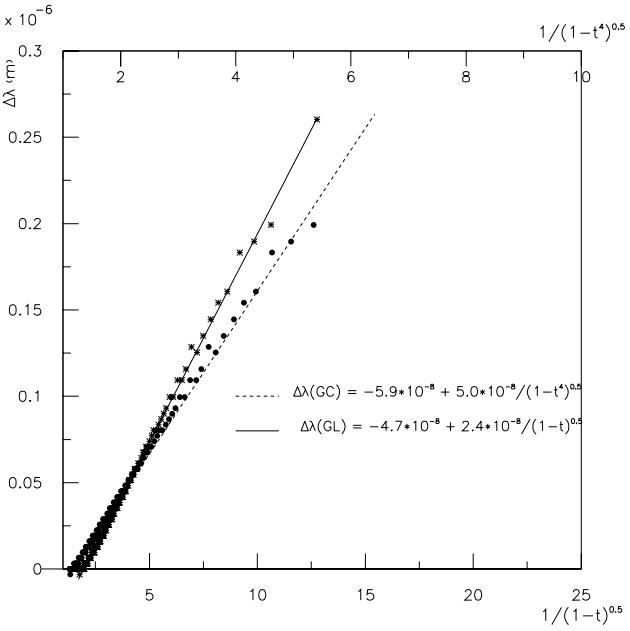

Figure 4: Effect of temperature on the relative magnetic penetration depth for $T_c = 9.3K$ [8] for cavity GEN1 ($\chi^2_{GL} = 1.58$ and $\chi^2_{GC} = 21.08$ respectively)

7 REFERENCES

[1] T.Yogi, G.J.Dick, J.E.Mercereau, Phys. Rev. Letters 39, (1977), pp826-829

[2] E.Kako et al. “Improvement of cavity performance by electropolishing in the 1.3GHz Nb superconducting cavities”, this conference

[3] V.L.Ginzburg and L.D.Landau, JETP 20 (1950), p1064.

[4] J.Bardeen, L.N.Cooper, J.R.Schrieffer, Phys.Rev. 108 (1957), pp1175-1204.

[5] H.Safa et al., “RRR Mapping of SRF cavities by a magnetometric method”, Proc. of 8^{th} SRF Workshop, Abano Terme, (1997).

[6] T. Junquera et al., “Thermal stability analysis of superconducting RF cavities”, Advances in Cryogenic Eng., Vol 43.

[7] T.Hays, H.Padamsee, “Measuring the RF critical fields of Pb, Nb, Nb_3Sn”, SRF 980804-06, LNS, Cornell Univ..

[8] M Cyrot and Davor Pavuna, “Introduction to superconductivity and High-Tc Materials”, (1992), p113.

[9] B.Bonin, “Materials for superconducting cavities”, CERN96-03, p194.

[10] M.Fouaidy, Private communication.

[11] C.Antoine et al., “Nuclear Microprobe studies of impurities segregation in Niobium used for radiofrequency cavities”, Proc. of 8^{th} SRF Workshop, Abano Terme, (1997).